

CIRPe 2015 - Understanding the life cycle implications of manufacturing  
Estimation of load history by residual stress relaxation

B. Breidenstein, B. Denkena, T. Mörke, R. Hockauf\*

*Institute of Production Engineering and Machine Tools, Leibniz Universität Hannover, 30823 Garbsen, Germany*

\* Corresponding author. Tel.: +49-511-762-4788 ; fax: +49-511-762-5115. E-mail address: [hockauf@ifw.uni-hannover.de](mailto:hockauf@ifw.uni-hannover.de)

---

**Abstract**

Focusing on the impact of machining on structural integrity and fatigue life of components the surface and subsurface properties are of major importance. It is well known that machining induced residual stresses have a significant influence on the fatigue life of a component. Due to thermal and mechanical loads during a product's life cycle these stresses relax, which is undesired in most cases.

The presented approach utilizes relaxations due to mechanical load to estimate the load history of a component. It is intended to qualify residual stress relaxation as a load sensor and to determine the limits of this approach. Therefore, it is demonstrated, how the residual stress state induced by turning of AISI 1060 determines the critical load causing relaxation. Subsequently, the influence of load stress and the number of load cycles is used to build up a model. The presented approach accesses load information from mass production components. Until now, this information is typically limited to prototypical developments or high price parts equipped with external sensors. One application of life cycle data is condition-based maintenance. This technology allows to extend service intervals and prevent a premature replacement of undamaged components. Thus, cost and resource efficiency are augmented. It is demonstrated that based on the changes of residual stress, possible mechanical loads and number of load cycle combinations can be identified. The changes are used to estimate the experienced loads.

© 2015 The Authors. Published by Elsevier B.V. This is an open access article under the CC BY-NC-ND license

(<http://creativecommons.org/licenses/by-nc-nd/4.0/>).

Peer-review under responsibility of the organizing committee of CIRPe 2015 - Understanding the life cycle implications of manufacturing

*Keywords:* Residual stress; Fatigue; Surface integrity

---

**1. Introduction**

The vision of the Collaborative Research Centre SFB 653 "Gentelligent Components in Their Lifecycle" includes technologies which enable components to store information about their own production and to self-monitor their condition [1, 2]. A special interest is directed towards sensing components that communicate their load history. Enabling future mass production components to give feedback based on real life application offers great potential for life cycle monitoring and maintenance planning as well as for design evolution regarding tailored adaptation to load. One key aspect is the possibility to determine whether and how a component has been loaded during the last maintenance interval and to estimate its failure possibility. The presented approach utilizes the changes of subsurface properties such as residual stress

relaxation and change of dislocation density during the component's lifecycle to estimate its load history.

The surface and subsurface properties are of significant importance since they affect directly a component's fatigue life and fracture behavior. The term surface integrity, acknowledged by Field and Kahles, summarizes typical surface characteristics such as plastic deformation, micro cracking and residual stress distribution [3]. A variety of results has been published on the effects of surface integrity on a component's behavior. Regarding residual stresses, it has been demonstrated that near surface compressive residual stress increases its fatigue life whereas tensile residual stress has a negative impact [4].

Starting in 1951 Henriksen investigated the surface integrity characteristics of components through an analysis of residual stress induced in machining processes [5]. One of the most common approaches is the measurement of residual stresses in

the near surface area by X-ray diffraction (XRD) and the  $\sin^2\psi$ -method [6]. As a result, residual stresses of the 1<sup>st</sup> order can be measured quantitatively, whereas 2<sup>nd</sup> order residual stresses are represented by the peak full width at half maximum (FWHM) and have to be regarded as a qualitative indicator.

The machining process, which is mostly the last step in the manufacturing chain has a significant influence on surface integrity of a work piece. In terms of cutting the mechanical deformation of material by the cutting edge leads to compressive residual stresses in the near surface area. The thermal load during the process in interaction with the rapid cooling after manufacturing causes tensile residual stresses [7]. In addition, finishing processes such as burnishing, deep rolling, shot peening or laser shock peening are available to specifically influence surface integrity.

Research on the influence of subsurface properties on fatigue life of a component shows that with decreasing ultimate strength of the material the influence of residual stresses on fatigue life decreases [8]. Below  $R_m < 1400$  MPa residual stresses in metallic components relax [8]. Relaxation is caused by mechanical and thermal load and depends on material properties such as yield strength, thus it depends on heat treatment. Their effects on lifetime are described independently. A thermal load of about 50 % of the melting temperature causes a significant relaxation of residual stresses. In most cases technical components do not reach those temperatures. At lower temperatures, the decrease is negligible [9, 10, 11]. Therefore, the presented approach focuses on the reconstruction of a component's load history using the residual stress relaxation caused by mechanical loads. A cyclic mechanical load scenario is characterized by the load amplitude and the number of load cycles. Extensive research for different materials and heat treatment conditions has been published. Experiments on AISI 4041 show an increasing residual stress relaxation for increasing load stress amplitude. The strongest relaxation appears during the first load cycles. The material's ultimate strength determines the residual stress sensitivity, which describes the degree of relaxation [8, 11, 12]. The effective stress in a component's surface area equals the superposition of load stress amplitude and residual stresses prior loading. Following the shell/core approach, relaxation is based on local plastic deformation [10]. For steel components the equivalent stress is expressed based on the von Mises criterion [8].

Even though a variety of publications on the change of subsurface properties due to fatigue has been published, there has been no utilization of these changes for an estimation of a component's load history. Based on the description of relaxation, the presented approach combines common approaches to identify load stress amplitudes and number of load cycles that cause a desired change of individual subsurface properties.

**2. Experimental setup**

AISI 1060 specimens are identically machined by turning to induce defined residual stresses. The residual stresses due to machining are used to set up critical load stresses, causing relaxation. Subsequently fatigue experiments are carried out

and the alteration of FWHM and the relaxation of residual stresses are monitored to generate data in order to empirically model the changes individually. The models are combined to identify the most likely combination of load stress and number of loads causing all monitored properties changes.

*2.1. Preparation and characterization of the specimens*

Machining processes significantly change a component's surface and subsurface properties. Literature results as well as earlier research of the publishing authors show that characteristics such as tensile and compressive residual stresses can be induced by turning with a high reducibility [13, 14]. Specimens for cyclic fatigue tests are machined on a Gildemeister CTX 520 L CNC lathe following DIN standard 50113 (smallest diameter 7 mm). Table 1 summarizes the applied tool geometry. The experiments are carried out applying a feed of  $f = 0.01$  mm at a cutting speed of  $v_c = 30$  m/min. The depth of cut is set to  $a_p = 0.1$  mm. Yield and ultimate strength ( $R_m = 830$  MPa,  $R_e = 440$  MPa) as well as yield point for compressive load ( $\sigma_{d0.2} = 454$  MPa) of AISI 1060 high carbon steel in the as received condition are experimentally determined.

Table 1: Tool geometry

tool geometry: SNMA-120408-S02020-MW			
tool cutting edge angle	$\kappa_r = 75^\circ$	tool orthogonal clearance angle	$\alpha_o = 5^\circ$
tool cutting edge inclination	$\lambda_s = -5^\circ$	tool orthogonal rake angle	$\gamma_o = -5^\circ$
rounded cutting edge radius	$r_p = 50 \mu\text{m}$	corner radius	$r_c = 0.8 \text{ mm}$

To characterize the subsurface condition after machining, residual stress measurements are carried out in  $\phi_A = 0^\circ, 45^\circ$  and  $90^\circ$  to the axial direction of the specimen determining the normal stresses  $\sigma_{xx}, \sigma_{xy}$  and  $\sigma_{yy}$ . Figure 1 illustrates the orientation of the mentioned stresses.

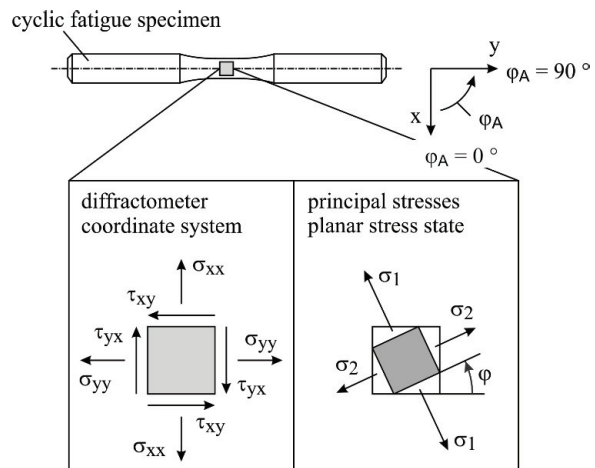


Fig. 1. Location and orientation of normal and shear stresses

Residual stresses of 2<sup>nd</sup> and 3<sup>rd</sup> order are qualitatively expressed by the width of the X-ray peak at its half maximum (FWHM). The determined values are mean values of the measurements carried out at  $\varphi_A = 0^\circ, 45^\circ$  and  $90^\circ$ . It is noted that various material properties e.g. chemical composition, phases, grain size and refinement, have a significant influence on the absolute value of FWHM. The latter can be influenced by machining. Therefore, the relative change rather than the absolute value is considered regarding the qualitative description of subsurface changes according to 2<sup>nd</sup> order residual stresses.

Analyzing 9 identically machined specimens directly after machining by X-ray diffraction and  $\sin^2\psi$ -method regarding normal and shear stresses as well as peak width (FWHM) shows high reducibility. Details are summarized in table 2 (for further details see [13]).

Table 2: Results of residual stress measurements directly after machining

residual stresses type I						type II & III			
$\sigma_{xx}$ (MPa)		$\sigma_{yy}$ (MPa)		$\tau_{xy}$ (MPa)		$\sigma_v^{**}$ (MPa)		FWHM ( $^\circ$ )	
$\mu$	s	$\mu$	s	$\mu$	s	$\mu$	s	$\mu$	s
-286	16	-348	32	-86	15	238	27	2.1624	0.054
$\mu$ = mean value, s = std. dev. (sample)									
* following Dölle [15], ** following von Mises [16]									

Assuming the case of plane stress, the assessment of normal and shear stresses allows the discretion of the full stress tensor. Thus, the equivalent stress  $\sigma_v$  can be determined.

## 2.2. Setup of fatigue experiments

The fatigue experiments are carried out using a rotating bending device type Zwick/Roell UBM 200 tC. A constant torque is applied on each specimen. The load case corresponds to a constant load stress distribution without mean stress ( $R = 1$ ). The setup is self-centering, whereby insufficient a linearity of the specimens could be compensated. The highest load stress is located at the specimen's surface. In case the superposition of load and residual stresses exceeds the yield strength of the material, the residual stresses relax due to yielding. A distinction must be made between quasi-static and cyclic loading.

## 3. Changes of subsurface states due to loading

Following the most common literature approach [17], the description of residual stress relaxation is separated in a quasi-static (number of loads  $0 < N \leq 1$ ) and a cyclic phase. The latter describes the relaxation for a number of load cycles  $N > 1$ . In both phases, an equivalent stress  $\sigma_v$  larger than the quasi static or a cyclic yield strength of the material ( $R_e^{stat}$  or  $R_e^{cycl}$ ) leads to residual stress relaxation.

As a consequence of the machining process, a plain residual stress state is present, which has to be taken into account determining the equivalent stress. Since the load stress is

applied in axial specimen direction, the superpositioning of residual and load stresses requires a transformation of the principal residual stresses into the specimen's coordinate system. Therefore, normal and shear stresses have to be taken into account. Provided that a uniaxial load stress  $\sigma_{load}$  in axial direction (y) is applied, the equivalent stress is described following the von Mises yield criteria equation.

$$\sigma_v = \sqrt{\sigma_{xx}^2 - \sigma_{xx}(\sigma_{yy} + \sigma_{load}) + (\sigma_{yy} + \sigma_{load})^2 + 3\tau_{xy}^2} \quad (1)$$

The critical load stress results for  $\sigma_v = R_e^{stat}$  or  $R_e^{cycl}$  to:

$$\sigma_{crit,load} = \frac{\sigma_{xx}}{2} - \sigma_{yy} \pm \frac{\sqrt{4 \cdot R_e^2 - 3 \cdot \sigma_{xx}^2 - 12 \cdot \tau_{xy}^2}}{2} \quad (2)$$

Considering the residual stresses of the machined specimens (table 2) the critical load stresses equal to  $\sigma_{crit,load}^{stat} = -115$  MPa respectively  $+549$  MPa and  $\sigma_{crit,load}^{cycl} = -204$  MPa respectively  $+617$  MPa. In both cases the compressive loading will cause relaxation.

### 3.1. Experimental results

Fatigue specimens are produced and the residual stress is determined according to the description above. Subsequently, fatigue experiments are carried out applying three different load stress amplitudes. Three identically machined specimens are used for each load stress amplitude to determine the influence of load stress and the number of load cycles on residual stress relaxation. Load stress amplitudes above the critical static stress (load stress 1) and above the critical cyclic stress (load stress 2) are applied. Additionally, a load stress of 80 % of the material's yield strength (load stress 3) is analyzed (see table 3). The residual stresses are determined after  $N = 1, 10, 100, 1000$  and  $10.000$  load cycles.

Table 3: Applied load stresses

Load stress 1	$\sigma_{load} = \pm 132$ MPa
Load stress 2	$\sigma_{load} = \pm 220$ MPa
Load stress 3	$\sigma_{load} = \pm 352$ MPa

Figure 2 depicts the residual stress relaxation for an increasing number of load cycles for the mentioned load stresses. A load stress slightly higher than the critical quasi-static load leads to a relaxation after the first load cycle. Successive load cycles do not cause significant relaxation. The residual stress relaxation in tangential (x) as well as in axial direction (y) increases with an increasing number of load cycles for loads above the critical cyclic load stress. With an increasing load, the quasi-static and cyclic relaxation increases as well. The quasi-static and cyclic relaxations follow a linear relation to the number of load cycles and the load stress.

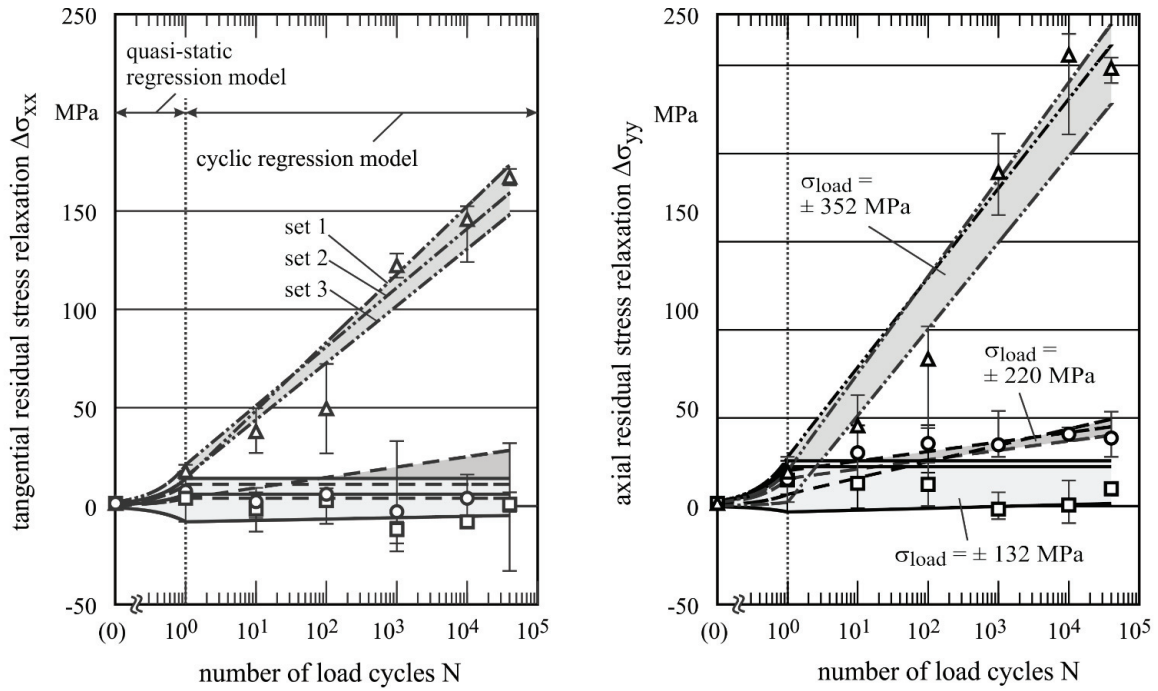


Fig. 2. Residual stress relaxation due to mechanical loading in tangential and in axial direction

3.2. Full width at half maximum

The full width at half maximum describes the width of the peak on the 2-theta scale in degrees. Among others, it correlates with the dislocation density and therefore the residual stresses type II and III. The fatigue experiments cause a different behavior of the full width at half maximum (FWHM) than the residual stresses. Figure 3 depicts that AISI 1060 shows no significant change of the FWHM due to the load stress amplitudes below  $\sigma_{load} = \pm 352 \text{ MPa} \approx 80 \% R_e$ . A linear decrease leading to  $\Delta FWHM = 0.3^\circ$  after  $N = 100.000$  load cycles is determined. A different behavior of residual stresses and FWHM allows the consideration of the FWHM building a model to reconstruct the load history of a component.

3.3. Quantification

To determine the load history of a component common equations by introduced by [17] are combined and resolved to determine possible combinations of load stress and number of load cycles leading to given residual stress and FWHM alterations. The approach is divided into quasi-static and cyclic behavior. At first, the results depicted in figure 2 and 3 are described according to Eq. 3. The quasi-static residual stress relaxation in axial and in tangential direction caused by the first load cycle ( $0 < N \leq 1$ ) are approximated linear to the load stress (Eq. 3).

$$\sigma_i(N) = \sigma_i(N=0) + b_i \cdot \sigma_{load} \cdot N \quad (3)$$

$\sigma_i(N=0)$  represents the initial value of residual stresses. The coefficient  $b_i$  is determined to describe the relaxed stress per load cycle depending on the amplitude of load stress. Exceeding the critical quasi-static load stress,  $b_i$  increases linear to the load stress amplitude (Eq. 4).

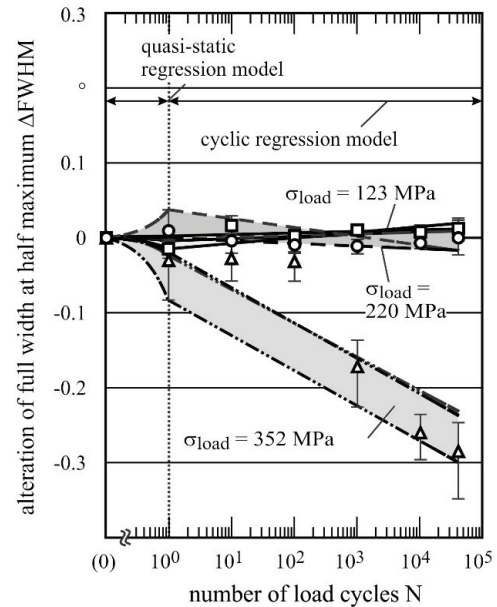


Fig. 3. Alteration of full width at half maximum due to mechanical loading in tangential and in axial direction

$$b_i(\sigma_{load}) = p_1 \cdot \sigma_{load} + p_2 \quad (4)$$

In the following, the corresponding influence of cyclic load ( $1 < N \leq 10^6$ ) is quantified by a logarithmic function presented by [17]. Based on the condition after the first cycle  $\sigma_i(N = 1)$  the relaxation is described in linear dependence to the logarithm of the number of load cycles (Eq. 5).

$$\sigma_i(N) = \sigma_i(N = 1) - A_i \cdot \sigma_{load} \cdot \log(N) \quad (5)$$

The coefficient  $A_i$  is determined to describe the cyclic relaxation per load cycle depending on the amplitude of load stress. Exceeding the critical cyclic load stress,  $A_i$  increases linear to the load stress amplitude (Eq. 6).

$$A_i(\sigma_{load}) = q_1 \cdot \sigma_{load} + q_2 \quad (6)$$

In addition to the relaxation of the residual stresses in axial and in tangential direction, the change of the full width at half maximum is quantified following the same procedure.

**4. Estimation of load history**

If the initial condition of a component is given, the residual stress relaxation and the alteration of FWHM can be determined. Presuming a number of load cycles greater  $N > 1$ , allows the combination of Eq. 3 and 5 equals Eq. 7.

$$\sigma_i(N) = \sigma_i(N = 0) + b_i \cdot \sigma_{load} - A_i \cdot \sigma_{load} \cdot \log(N) \quad (7)$$

Next the dependencies of  $b_i$  and  $A_i$  on the load stress considered by substituting the coefficients by Eq. 4 and 6. Since Eq. 3 and 5 are depending on two unknown elements, the individual equations as well as the combination cannot be resolved to determine a single possible solution. Infinite combinations of load stress and number of cycles can lead to specific changes. To quantify possible solutions, the resulting equation is resolved (Eq. 8).

$$N(\sigma_{load}) = \exp\left(\frac{\sigma_i(N = 0) - \Delta\sigma_i + \sigma_{load} \cdot (p_2 + \sigma_{load} \cdot p_1)}{q_2 + \sigma_{load} \cdot q_1}\right) \quad (8)$$

The proceeding is used for the residual stress in axial and tangential direction ( $\sigma_{yy}, \sigma_{xx}$ ) as well as for the FWHM. To illustrate the procedure the following initial condition and changes of subsurface properties are assumed:

Table 4: Changes of subsurface properties underlying figure 4

Residual stresses in tangential direction	$\Delta\sigma_{xx} = 113 \text{ MPa}$
Residual stresses in axial direction	$\Delta\sigma_{yy} = 189 \text{ MPa}$
Full width at half maximum	$\Delta\text{FWHM} = 0.16^\circ$

Figure 4 illustrates all possible combinations of load stress and number of load cycles causing the given changes of axial and tangential residual stresses (solid and dashed line) and FWHM (dashed/dotted line). The intersections represent possible combinations of interest, since the solution must be true for all properties.

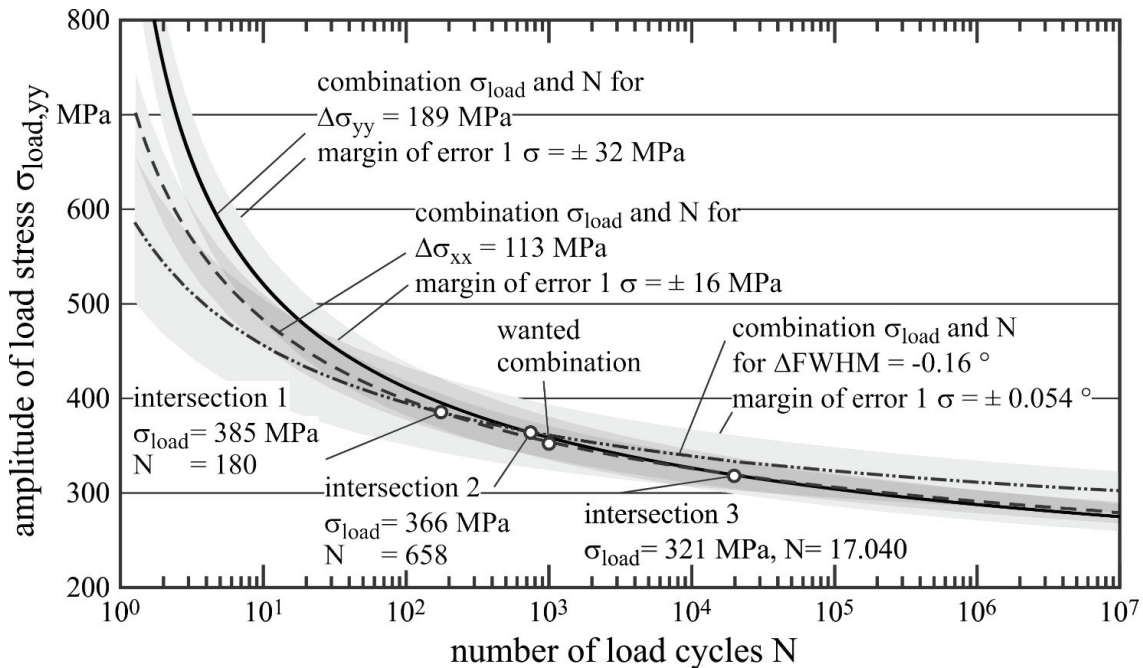


Fig. 4. Possible combinations of load stress and number of load cycles causing given change of residual stresses in axial and in tangential direction as well as FWHM



The assumed subsurface changes accrued due to a loading of  $\sigma_{load} = 352$  MPa and  $N = 1,000$ . Three intersections are found at  $\sigma_{load} = 385$  MPa and  $N = 180$ ,  $\sigma_{load} = 366$  MPa and  $N = 658$  and  $\sigma_{load} = 321$  MPa and  $N = 17,040$ . The model therefore over- or underestimates the load stress by +33 MPa or -30 MPa. Due to the logarithmic character of the underlying equations, the number of load cycles is over- or underestimated by +16,040 or -820.

Certain inaccuracies have to be taken into account to estimate the significance of the determined possible load cases. The deviation of the initial subsurface condition of the machined specimens is summarized in table 2. The measured deviation  $1\sigma$  between 16 MPa and 32 MPa or  $0.054^\circ$  is individually considered and illustrated in figure 4 by grey shading. The range of load cases expands from  $\sigma_{load} = 540$  MPa and  $N = 5$  to  $\sigma_{load} = 268$  MPa and  $N = 10^7$ . Due to the high uncertainty the possible combination of load cycles covers close to the full range of load cycles. The load amplitude is narrowed down to a range of about 272 MPa.

It is demonstrated that the presented approach is capable to determine loads above the critical load stress. The estimation of possible load stress amplitudes is significantly more precise than for the number of cycles. Next to the level of relaxation, the margin of error given by the reproducibility of initial subsurface condition after machining is substantial for the model's accuracy.

## Summary

A first step towards the realization of sensing components from mass production could be made by implementing the presented approach. The change of subsurface properties due to mechanical load is used to estimate the load history of a component. The residual stress relaxation and alteration of the FWHM due to fatigue load (rotating bending,  $R=1$ ) have been quantified for turned AISI 1060 steel specimens. Well accepted equations were combined and resolved to determine possible load cases leading to specific changes of single properties. To consider inaccuracy the deviation between identically machined specimens has been taken into account. The key information is summarized as followed:

- The approach requires quantification of residual stress relaxation behavior and alteration of FWHM.
- With increasing accuracy of relaxation models, experimental efforts could be substituted.
- Independent description of alternating subsurface properties allows identification of possible load cases.
- Intersections of solutions mark most likely load histories.
- Load stress amplitudes above the critical quasi-static and cyclic load stress are necessary.
- Accuracy decreases, if load amplitude or number of cycles is too small for single subsurface properties to change.
- In worst-case scenarios, it is necessary to consult further data. For application worst-case regarding to fatigue life or operational stability.
- A fundamental, still unsolved prerequisite for launching the method in industry is the fast measurement of residual stresses in a shop floor environment before, during and after a components usage.

## Acknowledgements

The presented investigations were undertaken with support of the German Research Foundation (DFG) within the Collaborative Research Centre (CRC) 653. We thank the DFG for its financial and organizational support of this project. We also acknowledge that the fatigue experiments and parts of the material characterisation were supported by the Institute of Materials Science of the Leibniz Universität Hannover.

## References

- [1] Denkena B, Henning H, Lorenzen LE. Genetics and intelligence: New approaches in production engineering. *Prod. Eng.* 2010;4:65–73
- [2] Denkena B, Mörke T, Krüger M, Schmidt J, Boujnah H, Meyer J, P. Gottwald, B. Spitschan, M. Winkens. Development and first applications of gentelligent components over their lifecycle. *JMST* 2014 7(2);139–150
- [3] Field M, Kahles JF. The surface integrity of machined and ground high strength steels. *DMIC Report* 1964 210;54–77
- [4] Withers PJ. Residual stress and its role in failure. *Reports on Progress in Physics* 2007 70(12);2211–2264
- [5] Henriksen EK. Residual stresses in machined surfaces. *Transactions of the ASME* 1951 73;69–74
- [6] Macherauch E, Müller P. Das  $\sin^2\psi$ -Verfahren der röntgenographischen Spannungsmessung. *Zeitschrift für Angewandte Physik* 1961 13:305–312
- [7] Macherauch E, Wohlfahrt U, Wolfstieg. Zur zweckmäßigen Definition von Eigenspannungen. *Härterei-Tech. Mitt.* 1973 28;201–211
- [8] Macherauch E, Wohlfahrt H. Eigenspannungen und Ermüdung. In: *Ermüdungsverhalten metallischer Werkstoffe*. DGM-Informationsgesellschaft Verlag 1985;237–283
- [9] M'Saoubi R, Outeiro JC, Chandrasekaran H, Dillon Jr OW, Jawahir IS. A review of surface integrity in machining and its impact on functional performance and life of machined products. *IJSM* 2008;1(1–2):203–236
- [10] Vöhringer O, Wohlfahrt H. Abbau von Eigenspannungen. In: Hauk V, Macherauch E, editors. *Eigenspannungen und Lastspannungen, Moderne Ermittlung, Ergebnisse, Bewertung*. München: Carl Hanser Verlag; 1982, 49–83
- [11] Schulze V. Modern mechanical surface treatment. States, stability, effects. 1st ed. Weinheim: Wiley-Verlag; 2006
- [12] Scholtes B. Eigenspannungen in mechanisch randschichtverformten Werkstoffzuständen, Ursachen-Ermittlung-Bewertung. 1st ed. Oberursel: DGM-Informationsgesellschaft; 1990.
- [13] Denkena B, Köhler J, Breidenstein B, Mörke T. Elementary studies on the inducement and relaxation of residual stress. *Procedia Engineering* 2011 19; 88–93
- [14] Denkena B, Breidenstein B, Reimche W, Mroz G, Mörke T, Maier HJ. Changes of Subsurface Properties due to Fatigue Determined by  $\sin^2\psi$ -method and Harmonic Analysis of Eddy Current Signals. *Procedia Technology* 2014;15:503–513.
- [15] Dölle H, Hauk V. Röntgenographische Spannungsermittlung für Eigenspannungssysteme allgemeiner Orientierung. *Härterei-Tech. Mitt.* 1976 31; 165–168
- [16] von Mises R. Mechanik der festen Körper im plastisch deformablen Zustand. *Göttin. Nachr. Math. Phys.* 1913 1;582–592
- [17] Kodama S. The Behaviour of Residual Stress during Fatigue Stress Cycles. In: *Society of Materials Science Japan* (Hg.), Mechanical Behavior of Materials - Vol. 2 Fatigue of Metals. 1972 2:111–118. 1972.